Journal of Alloys and Compounds 509 (2011) 2602–2605

Contents lists available at ScienceDirect

Journal of Alloys and Compounds

journal homepage: www.elsevier.com/locate/jallcom

Large reversible magnetocaloric effect in Er_2In compound

H. Zhang[a,*], B.G. Shen[a], Z.Y. Xu[a], J. Chen[a], J. Shen[b], F.X. Hu[a], J.R. Sun[a]

[a] State Key Laboratory for Magnetism, Institute of Physics, Chinese Academy of Sciences, Beijing 100190, People's Republic of China
[b] Technical Institute of Physics and Chemistry, Chinese Academy of Sciences, Beijing 100190, People's Republic of China

ARTICLE INFO

Article history:
Received 12 August 2010
Received in revised form
12 November 2010
Accepted 15 November 2010
Available online 23 November 2010

Keywords:
Rare-earth intermetallic compound
X-ray diffraction
Magnetocaloric effect

ABSTRACT

The magnetic properties and magnetocaloric effects (MCEs) of the Er_2In compound have been investigated. It is found that Er_2In undergoes a second-order magnetic transition from ferromagnetic (FM) to paramagnetic (PM) state at the Curie temperature $T_C = 46$ K and no other transition is observed. These observations are in consistent with previously published works. For a magnetic field change from 0 to 5 T, the maximum magnetic entropy change (ΔS_M) and refrigerant capacity (RC) are −16 J/kg K and 490 J/kg, respectively, which are comparable to or larger than those of some magnetic refrigerant materials with first-order magnetic transition around the similar magnetic ordering temperature. Large reversible MCE and high RC value indicate that the Er_2In compound is a suitable candidate of magnetic refrigerants in low temperature range.

1. Introduction

Since the discovery of the giant magnetocaloric effect (MCE) in $Gd_5(Si_{1-x}Ge_x)_4$ [1], a great deal of effort has been devoted to research on magnetic refrigerant materials. This is because magnetic refrigeration, based on the MCE, is expected to be a potential alternative to conventional vapor compression refrigeration due to its energy-efficiency and environment-friendly features [1–4]. The MCE can be characterized by the magnetic entropy change (ΔS_M) and/or adiabatic temperature change (ΔT_{ad}). Besides, the refrigerant capacity (RC) has been considered as another important parameter to quantify the magnetocaloric properties [5,6], because the ΔS_M does not sufficiently identify the potential of a magnetic refrigerant material. In the past decades, a great number of magnetic materials with large MCEs have been reported [7–10]. Among these studies, much attention was focused on refrigerant materials undergoing a first-order magnetic transition (FOMT) because of their large MCEs around the magnetic transition temperatures [11–14]. Unfortunately, the first-order phase transition is usually accompanied by considerable thermal and magnetic hystereses, which may reduce the RC of magnetic materials [15,16]. Recently, reductions of hysteresis associated with FOMT were reported in some magnetic refrigerant materials [6,17]. For example, the thermal and magnetic hystereses of the $Gd_5Si_{1.8}Ge_{1.8}Sn_{0.4}$ ribbons were reduced significantly with the melt-spun technique [17]. By the partial substitution of Mn for Fe, a large depression of hysteresis was achieved in La(Fe, Si)$_{13}$-based compounds [6]. However, it was also found that the improvement of hysteresis always accompanies the weakening of MCEs of the materials. On the other hand, some materials with the second-order magnetic transition (SOMT), such as ErGa [18], $R_6Co_2Si_3$ [19], Pr_5Si_3 [20], and $(Gd_{1-x}Dy_x)_3Al_2$ [21], were reported to exhibit large reversible MCEs as well as high RC values over a wide temperature region. Consequently, from an application point of view, it is of importance to explore magnetic refrigerant materials with large reversible MCEs and high RC based on SOMT. In addition, it is known that materials exhibiting large MCEs below 70 K can be used in a magnetic refrigerator to liquefy hydrogen gas [4]. Based on this concept, it is highly desirable to develop new magnetic materials applicable in a low temperature range.

R_2In compounds, where R is a rare-earth metal, have been studied extensively in previous works [22–25]. All these compounds are isomorphous and crystallize in a Ni_2In-type hexagonal structure with space group $P6_3/mmc$. These compounds show a great variety of magnetic properties depending on the rare earth. At high temperature, the susceptibilities of all compounds except Sm_2In follow the Curie–Weiss law with a large and positive paramagnetic Curie temperature. Based on the investigations of neutron diffraction and Mössbauer spectroscopy, Ravot et al. reported that Er_2In compound undergoes ferromagnetic ordering below the Curie temperature $T_C = 40$ K: the saturated moments at both the Er^{3+} sites are 8.0 μ_B and they lie close to the basal plane [24].

Recently, it has been reported that the R_2In (R = Tb, Dy and Ho) compounds show large reversible MCEs over a wide temperature region associated with SOMT [26–30]. In the present work, we have carried out further investigation on the magnetic and magne-

* Corresponding author at: State Key Laboratory of Magnetism, Institute of Physics, Chinese Academy of Sciences, P.O. Box 603, Beijing 100190, People's Republic of China. Tel.: +86 10 82648085; fax: +86 10 82649485.
E-mail address: zhanghuxt@gmail.com (H. Zhang).

0925-8388/$ – see front matter © 2010 Elsevier B.V. All rights reserved.
doi:10.1016/j.jallcom.2010.11.108

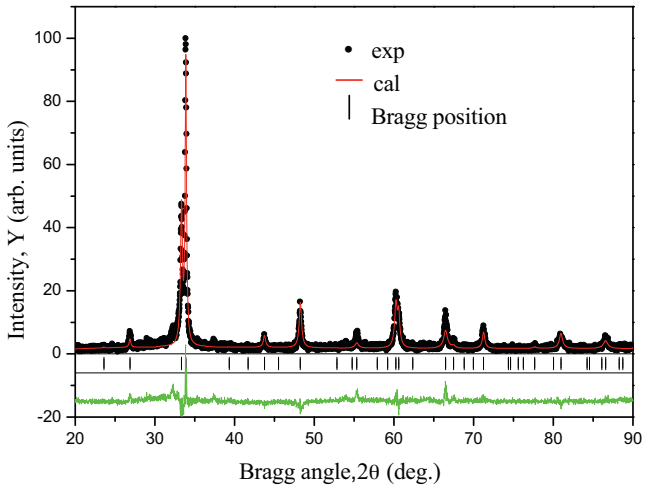

Fig. 1. The observed (dots) and calculated intensities (line drawn through the data points) of the fully refined powder diffraction pattern of Er_2In compound. The short vertical lines indicate the calculated positions of the Bragg peaks of the hexagonal Ni_2In-type crystal structure. The lower curve shows the difference between the observed and calculated intensities.

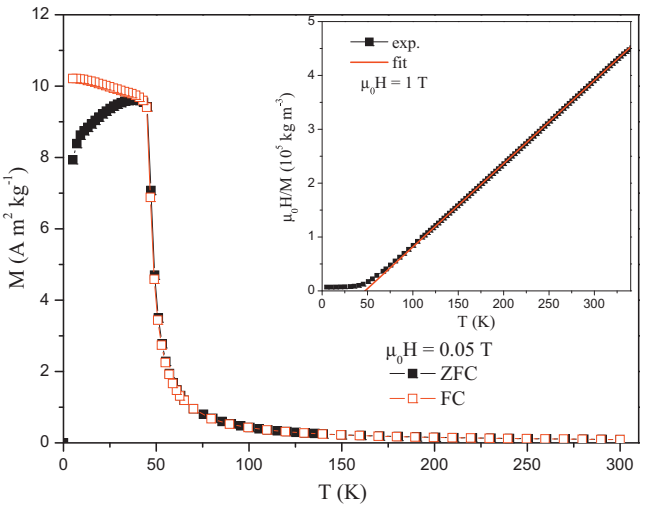

Fig. 2. Temperature dependencies of the ZFC and FC magnetizations for Er_2In compound under a magnetic field of 0.05 T. The inset shows the temperature variation of ZFC inverse susceptibility fitted to the Curie–Weiss law under 1 T.

tocaloric properties of Er_2In. This compound with a SOMT is found to exhibit a large reversible ΔS_M and a high RC value around T_C.

2. Experimental

The Er_2In ingot was prepared in a purified Ar atmosphere by arc-melting of the stoichiometric amounts of the high purity (>99.9 wt.%) constituent elements on a water cooled copper hearth. To achieve compositional homogeneity, the obtained ingot was wrapped in a molybdenum foil, sealed in a high-vacuum quartz tube, annealed for 100 h at 1073 K and then quenched into liquid nitrogen. The phase structure and the crystal lattice parameters were examined by the Rietveld refinement of the room-temperature X-ray powder diffraction data collected using the Cu Kα radiation. The magnetic properties were measured by employing a physical property measurement system (PPMS) from Quantum Design Inc.

3. Results and discussion

Fig. 1 shows the X-ray diffraction (XRD) pattern of Er_2In at room temperature and Rietveld refinement to the experimental data. The refinement shows that the compound crystallizes in a single phase with a hexagonal Ni_2In-type structure (space group $P6_3/mmc$). The lattice parameters a and c are determined to be 5.2909(6) and 6.6373(9) Å, respectively, which are in a good agreement with the data in previous report [23].

The temperature (T) dependencies of zero-field-cooling (ZFC) and field-cooling (FC) magnetizations (M) have been obtained under a magnetic field of 0.05 T and the results are shown in Fig. 2. The Er_2In compound exhibits a ferromagnetic (FM)–paramagnetic (PM) transition at Curie temperature T_C = 46 K, corresponding to the minimum of dM/dT curve. No thermal hysteresis was observed in the ZFC and FC curves above T_C. However, it is noted that the ZFC and FC magnetization data show thermomagnetic irreversibility below T_C as observed in previous work [24]. This is likely due to a domain wall pinning effect. The inverse dc magnetic susceptibility of Er_2In was measured in a field of 1 T and the Curie–Weiss fit to it is shown in the inset of Fig. 2. The susceptibility above the ordering temperature obeys the Curie–Weiss law with an effective moment μ_{eff} = 9.60 μ_B/Er^{3+} and a PM Curie temperature θ_P = 47.2 K. The μ_{eff} determined from the fit is in a good agreement with the Er^{3+} free ion value of 9.59 μ_B. In addition, the positive value of PM Curie temperature reveals that the Er_2In predominantly possesses FM interaction.

The magnetization isotherms of Er_2In were measured in a wide temperature range with different temperature steps in applied fields up to 5 T as shown in Fig. 3. Below T_C, the magnetization increases rapidly at low fields and shows a tendency to saturate with an increase of the field, confirming the typical nature of FM interaction. Besides, the M–H curves were measured around T_C in field increasing and decreasing modes to investigate the reversibility of the magnetic transition for Er_2In. It is clearly seen that there is no magnetic hysteresis upon changing the field direction, suggesting the magnetic transition of Er_2In is perfectly magnetic reversible, which is preferable for practical applications of the magnetic refrigerant materials. Fig. 4 shows the Arrott plots of Er_2In near T_C. It is well known that a magnetic transition is expected to be FOMT when the slope of the Arrott curve is negative; otherwise it will be SOMT when the slope is positive [31]. There are neither negative slopes nor inflection points, proving that the Er_2In is of SOMT.

The ΔS_M of Er_2In was calculated from the magnetization data using the Maxwell relation $\Delta S_M = \int_0^H (\partial M/\partial T)_H dH$ [32]. Fig. 5 displays the temperature dependencies of the $-\Delta S_M$ for different magnetic field changes. The maximum value of $-\Delta S_M$ is found to increase linearly with the increase of applied magnetic field and reaches a value of 16 J/kg K for a 0–5 T field change, which is comparable to or much larger than those of some magnetocaloric materials with the similar phase transition temperature, such as Dy_3Co (13.9 J/kg K at 44 K) [33], TbNiAl (13.8 J/kg K at 47 K) [34],

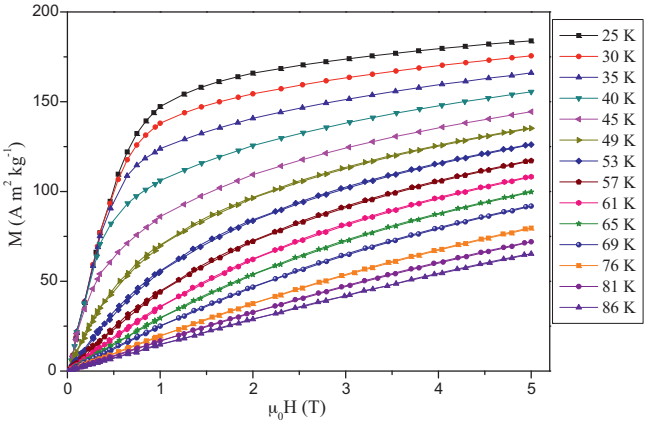

Fig. 3. Isothermal magnetization curves of Er_2In in a temperature range from 25 to 86 K.

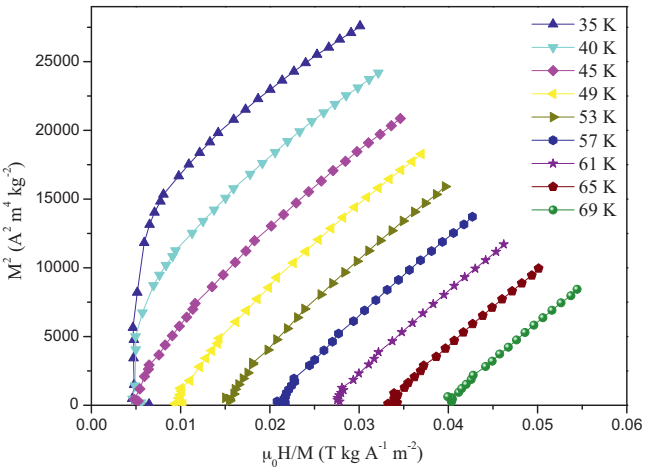

Fig. 4. Arrott plots of Er_2In at different temperatures near T_C.

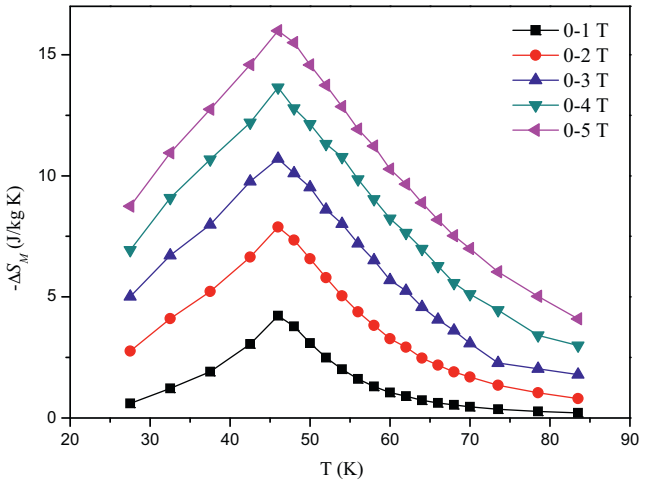

Fig. 5. The temperature dependencies of magnetic entropy change of Er_2In for different magnetic field changes.

$DyMn_2Ge_2$ (13.4 J/kg K at 40 K) [35], $GdAl_2$ (7.2 J/kg K at 44 K) [36], and Dy_5Ge_4 (6.8 J/kg K at 46 K) [37].

As another important criterion to evaluate the magnetic refrigerant materials, the RC of Er_2In compound was estimated based on the ΔS_M vs. T curves using the approach suggested by Gschneidner et al. [5]. The RC value is defined as $RC = \int_{T_1}^{T_2} |\Delta S_M| dT$, where T_1 and T_2 are the temperatures corresponding to both sides of the half-maximum value of $|\Delta S_M|$ peak, respectively. The calculation shows that the RC for Er_2In is 490 J/kg with T_1 = 25.5 K (temperature of the cold end) and T_2 = 66.5 K (temperature of the hot end) for a magnetic field change of 0–5 T. For comparison, Table 1 lists

Table 1
The main parameters regarding the MCEs for Er_2In and the representative refrigerant materials with working temperature around 46 K.

Materials	T_{ord} (K)	$-\Delta S_M$ (5 T) (J/kg K)	RC (5 T) (J/kg)	Refs.
$ErCo_2$	35	33.0	270[a]	[14]
Dy_3Co	44	13.9	498	[33]
TbNiAl	47	13.8	494	[34]
$DyMn_2Ge_2$	40	13.4	214[a]	[35]
$GdAl_2$	44	7.2	290[a]	[36]
Dy_5Ge_4	46	6.8	161[a]	[37]
Er_2In	46	16.0	490	This work

[a] The RC values are estimated from the temperature dependencies of ΔS_M in the reference literature.

Table 2
The main parameters regarding the MCEs for R_2In (R = Tb, Dy, Ho and Er) compounds.

Materials	T_C (K)	$-\Delta S_M$ (2 T) (J/kg K)	$-\Delta S_M$ (5 T) (J/kg K)	RC (5 T) (J/kg)	Refs.
Tb_2In	165	3.5	6.6	488[a]	[26]
Dy_2In	130	4.6	9.2	545[a]	[27]
Ho_2In	85	5.0	11.2	360	[29]
Er_2In	46	7.9	16.0	490	This work

[a] The RC values are estimated from the temperature dependencies of ΔS_M in the reference literature.

the magnetocaloric properties of Er_2In and some other magnetic refrigerant materials with a similar magnetic ordering temperature. Although the $ErCo_2$ compound with FOMT exhibits a large ΔS_M (−33 J/kg K) around T_C = 35 K [14], its RC value is smaller than that of Er_2In. The high RC of Er_2In is due to relatively broad distribution of ΔS_M peak. Table 2 summarizes the magnetocaloric properties of Er_2In and other R_2In (R = Tb, Dy and Ho) compounds with different Curie temperatures. It is noted that Er_2In exhibits the largest ΔS_M and a comparable RC value, while it also has the lowest T_C in this series of compounds. It has been pointed out that the working temperature and temperature span of the MCE could be tuned by replacing Er by Tb, Dy, or Ho [23,26,38]. Therefore, Er_2In and its descendants are expected to be good candidates for the magnetic refrigeration at low temperatures.

4. Conclusions

In summary, magnetic and magnetocaloric properties of Er_2In compound have been studied in detail. It shows that the compound possesses a FM–PM transition at T_C = 46 K, which is in a good agreement with previous works. The analysis of Arrott plot justifies that the magnetic transition is of second-order. For a magnetic field change of 0–5 T, a large value of $-\Delta S_M$ (16 J/kg K) is observed around T_C of Er_2In. Moreover, the RC for Er_2In is as high as 490 J/kg due to the large MCE over a wide temperature span, which is comparable to or larger than those of some magnetic refrigerant materials with FOMT around the similar magnetic ordering temperature. The large ΔS_M as well as the high RC value with no hysteresis loss are the advantages of Er_2In compound.

Acknowledgement

This work was supported by the National Basic Research Program of China, the National Natural Science Foundation of China, and the Knowledge Innovation Project of the Chinese Academy of Sciences.

References

[1] V.K. Pecharsky, K.A. Gschneidner Jr., Phys. Rev. Lett. 78 (1997) 4494.
[2] C.B. Zimm, A. Jastrab, A. Sternberg, V.K. Pecharsky, K.A. Gschneidner Jr., M. Osborne, I. Anderson, Adv. Cryog. Eng. 43 (1998) 1759.
[3] A.M. Tishin, in: Y.I. Spichkin (Ed.), The Magnetocaloric Effect and its Applications, Institute of Physics Publishing, Bristol, 2003.
[4] K.A. Gschneidner Jr., V.K. Pecharsky, A.O. Tsokol, Rep. Prog. Phys. 68 (2005) 1479.
[5] K.A. Gschneidner Jr., V.K. Pecharsky, A.O. Pecharsky, C.B. Zimm, Mater. Sci. Forum 315–317 (1999) 69.
[6] Z.P. Lin, S.D. Li, M.M. Liu, J.G. Duh, K. Peng, X.Y. Mao, J. Alloys Compd. 489 (2010) 1.
[7] D.M.R. Kumar, M.M. Raja, R. Gopalan, R. Balamuralikrishnan, A.K. Singh, V. Chandrasekaran, J. Alloys Compd. 461 (2008) 14.
[8] C. Jing, J.P. Chen, Z. Li, Y. Qiao, B.J. Kang, S.X. Cao, J.C. Zhang, J. Alloys Compd. 475 (2009) 1.
[9] H. Zhang, Y. Long, Q. Cao, Ya. Mudryk, M. Zou, K.A. Gschneidner Jr., V.K. Pecharsky, J. Magn. Magn. Mater. 322 (2010) 1710.
[10] H. Zhang, Ya. Mudryk, Q. Cao, V.K. Pecharsky, K.A. Gschneidner Jr., Y. Long, J. Appl. Phys. 107 (2010) 013909.
[11] Z.W. Ouyang, J. Appl. Phys. 108 (2010) 033907.
[12] B.G. Shen, J.R. Sun, F.X. Hu, H.W. Zhang, Z.H. Cheng, Adv. Mater. 21 (2009) 4545.

[13] N.V.R. Rao, R. Gopalan, V. Chandrasekaran, K.G. Suresh, J. Alloys Compd. 478 (2009) 59.
[14] N.K. Singh, P. Kumar, K.G. Suresh, A.K. Nigam, A.A. Coelho, S. Gama, J. Phys.: Condens. Matter. 19 (2007) 036213.
[15] V. Provenzano, A.J. Shapiro, R.D. Shull, Nature (London) 429 (2004) 853.
[16] E. Yüzüak, B. Emre, A. Yücel, Y. Elerman, J. Alloys Compd. 476 (2009) 929.
[17] T.B. Zhang, Y.G. Chen, Y.B. Tang, J. Phys. D: Appl. Phys. 40 (2007) 5778.
[18] J. Chen, B.G. Shen, Q.Y. Dong, F.X. Hu, J.R. Sun, Appl. Phys. Lett. 95 (2009) 132504.
[19] J. Shen, Y.X. Li, J.R. Sun, J. Alloys Compd. 476 (2009) 693.
[20] G. Tian, H.L. Du, Y. Zhang, Y.H. Xia, C.S. Wang, J.Z. Han, S.Q. Liu, J.B. Yang, J. Alloys Compd. 496 (2010) 517.
[21] Z.D. Han, P. Zhang, B. Qian, X.F. Jiang, D.H. Wang, J. Chen, J.F. Feng, Y.W. Du, J. Alloys Compd. 504 (2010) 310.
[22] H. Gamari-Seale, T. Anagnostopoulos, J.K. Yakinthos, J. Appl. Phys. 50 (1979) 434.
[23] W. Bazela, A. Szytula, J. Less-Common Met. 138 (1988) 123.
[24] D. Ravot, O. Gorochov, T. Roisnel, G. André, F. Bourée, J.A. Hodges, J. Magn. Magn. Mater. 128 (1993) 267.
[25] D. Ravot, O. Gorochov, T. Roisnel, G. Andre, F. Bouree-Vigneron, J.A. Hodges, Int. J. Mod. Phys. B 7 (1993) 818.
[26] Q. Zhang, J.H. Cho, J. Du, F. Yang, X.G. Liu, W.J. Feng, Y.J. Zhang, J. Li, Z.D. Zhang, Solid State Commun. 149 (2009) 396.
[27] Q. Zhang, X.G. Liu, F. Yang, W.J. Feng, X.G. Zhao, D.J. Kang, Z.D. Zhang, J. Phys. D: Appl. Phys. 42 (2009) 055011.
[28] A. Bhattacharyya, S. Chatterjee, S. Giri, S. Majumdar, J. Magn. Magn. Mater. 321 (2009) 1828.
[29] Q. Zhang, J.H. Cho, B. Li, W.J. Hu, Z.D. Zhang, Appl. Phys. Lett. 94 (2009) 182501.
[30] A. Bhattacharyya, S. Chatterjee, S. Giri, S. Majumdar, Eur. Phys. J. B 70 (2009) 347.
[31] S.K. Banerjee, Phys. Lett. 12 (1964) 16.
[32] V.K. Pecharsky, K.A. Gschneidner Jr., J. Appl. Phys. 86 (1999) 565.
[33] J. Shen, J.L. Zhao, F.X. Hu, G.H. Rao, G.Y. Liu, J.F. Wu, Y.X. Li, J.R. Sun, B.G. Shen, Appl. Phys. A 99 (2010) 853.
[34] N.K. Singh, K.G. Suresh, R. Nirmala, A.K. Nigam, S.K. Malik, J. Magn. Magn. Mater. 302 (2006) 302.
[35] H. Wada, Y. Tanabe, K. Hagiwara, M. Shiga, J. Magn. Magn. Mater. 218 (2000) 203.
[36] P. Kumar, K.G. Suresh, A.K. Nigam, J. Phys. D: Appl. Phys. 41 (2008) 105007.
[37] V.V. Ivtchenko, V.K. Pecharsky, K.A. Gschneidner Jr., Adv. Cryog. Eng. 46 (2000) 405.
[38] A. Szytula, R. Zach, J. Less-Common Met. 141 (1988) L5.